



# Standardizing thermal contrast among local climate zones at a continental scale: Implications for cool neighborhoods

Xuan Chen<sup>a</sup>, Jiachuan Yang<sup>a,\*</sup>, Chao Ren<sup>b</sup>, Sujong Jeong<sup>c</sup>, Yuan Shi<sup>d</sup>

<sup>a</sup> Department of Civil and Environmental Engineering, The Hong Kong University of Science and Technology, Hong Kong, China

<sup>b</sup> Faculty of Architecture, The University of Hong Kong, Hong Kong, China

<sup>c</sup> Department of Environmental Planning, Graduate School of Environmental Studies, Seoul National University, Seoul, South Korea

<sup>d</sup> Institute of Future Cities, The Chinese University of Hong Kong, Hong Kong, China

## ARTICLE INFO

### Keywords:

Local climate zone  
Microclimate  
Seasonal thermal contrast  
Urban heat island

## ABSTRACT

The Local Climate Zone (LCZ) classification system provides a standardized framework to differentiate neighborhoods for intra-city heat island studies. Yet the thermal contrast of air temperatures over different LCZs has not been examined at a continental scale. Using ground-based meteorological observations in 2016, here we investigated the seasonal thermal behaviors of various LCZs over China. Measured air temperatures over studied LCZs are found to have strong relations with latitude, altitude, and the distance to coastline. Thermal contrasts reduce to less than 1 °C in all seasons after removing the signal of background mean air temperature determined by geographical conditions. Despite the air temperature variation within individual LCZs, results reveal consistent characteristic air temperature regimes of LCZs exist at a continental scale. The warmth of built type LCZs is more evident at night, with an annual mean air temperature difference of 0.51 °C compared to the low plant LCZ. Among the studied LCZs, compact mid-rise neighborhoods have consistently high air temperatures throughout the year. Comparative analysis suggests that open high-rise neighborhoods are preferred over compact mid-rise and low-rise neighborhoods for sustainable city development. Our results provide useful guidance for landscape design and planning to create cool cities and neighborhoods.

## 1. Introduction

Land use/land cover conditions have significant impacts on local and regional meteorological variables. One of the most evident examples is the canopy urban heat island (UHI) effect, where urbanization leads to higher air temperatures in cities compared to their surrounding countryside [1]. Study of this phenomenon can be traced back to 1806, when Luke Howard observed higher daily air temperatures in London than in surrounding areas [2]. Elevated air temperatures in cities have adverse impacts on building energy consumption and public health during hot periods [3,4], and past decades have seen increasing UHI studies around the world [5–8]. In particular, extensive efforts have been devoted to seeking and implementing effective mitigation strategies for canopy UHIs to create cool cities [9–13]. The widely used canopy UHI intensity, defined as the urban-rural air temperature difference, is nevertheless sensitive to the selection of ‘urban’ and ‘rural’ sites [14,15]. Meanwhile, large intra-urban climate variability between neighborhoods has been reported for various cities, which were first derived from measuring

trips in early 1900s [16–18] (see Table 3 in Ref. [19]) and revealed in details by dense meteorological networks in recent years [20,21]. To better link local climate with built landscape properties, Stewart and Oke [22] developed the Local Climate Zone (LCZ) classification system that included ten built types and seven land cover types. Each LCZ type has distinguished features of surface cover, structure, material, and human activities, and has a unique characteristic air temperature regime that is most pronounced on dry, calm, and clear nights [22].

The LCZ system provides an objective framework for neighborhood-scale air temperature studies in different cities. Studies have adopted the LCZ scheme with in-situ measurements to assess the intra-urban air temperature variability in many metropolitan areas, including Hong Kong, Vancouver, Nagoya, Uppsala, Berlin, Londrina and Phoenix [23–27]. Reported thermal contrasts among various LCZs in studied cities evaluated the validity of the LCZ classification system, but the analysis of air temperature was mostly conducted at the city scale for a short study period. For example, Alexander and Mills [28] studied the relationship between air temperature and LCZ in Dublin for one week.

\* Corresponding author.

E-mail address: [cejcyang@ust.hk](mailto:cejcyang@ust.hk) (J. Yang).

<https://doi.org/10.1016/j.buildenv.2021.107878>

Received 24 February 2021; Received in revised form 3 April 2021; Accepted 6 April 2021

Available online 13 April 2021

0360-1323/© 2021 Elsevier Ltd. All rights reserved.

Shi et al. [29] used mobile measurements to estimate the air temperature differences between built type LCZ types on 13 individual days in Hong Kong. Although these studies provide useful information on thermal contrasts between neighborhoods within a city, a considerable difference is usually found in the results at different cities. For instance, the annual mean nocturnal air temperature of open midrise neighborhoods (LCZ 5) is about 4.4 °C higher than that of rural areas with low plants (LCZ D) under ideal days in Szeged, Hungary [30], but this difference is less than 1 °C in Nanjing, China [31]. This naturally leads to the question that whether the inconsistent thermal contrasts are caused by the air temperature variability of individual LCZ or by the geographical and climatic conditions in different cities. Such a question can only be achieved through large-scale analysis because geographical and climatic conditions are nearly identical at the city scale. A recent systematic review by Stewart [32] pointed out that one reason for the inconsistent thermal contrast could be the difference in measurement method and/or experimental design among various studies. Reporting metadata of instrumentation and field site characteristics is thus critical for heat island studies [33]. Note that many cities cannot afford a dense sensor network to understand their intra-urban temperature variation, and thus generalizable findings from a large-scale study based on the LCZ framework are needed to support cool neighborhood development in these cities.

Over a large spatial extent, geographical conditions and atmospheric forcing vary significantly and play essential roles in regulating meteorological variables. Wienert and Kuttler [34] found the dependence of urban-rural air temperature difference on latitude and suggested a larger maximum canopy UHI intensity in high-latitude regions. Thermal contrasts among different LCZs can change from city to city as the local landscape only contributes partially to determine the air temperature. Lowry [35] suggested that the difference in a meteorological variable between two places consisted of the background climate difference, the landscape effect (e.g., topography, shoreline), and the urban effect. The classification of urban land use into sub-categories by the LCZ scheme essentially targets a refined quantification of the urban effect in Lowry's framework. Following the concept of the LCZ scheme, the impact of local landscape on air temperature needs to be distinguished from those of background climate and landscape. A unique thermal contrast depending only on LCZ types, if existing over different climate types or/and topography, will be highly valuable for urban planning as it provides references for a variety of cities. The LCZs with low thermal contrasts against the others are cool neighborhoods that cities shall prioritize in their development plans for adapting to heat challenges. Researchers are starting to explore the implications of the LCZ scheme for various aspects of environmental sustainability at the city scale, including heat stress [36,37], energy demand [13], and ventilation [38]. To compare and unify the findings at different cities, it is necessary to standardize the thermal contrasts among LCZs over a large spatial extent through a new methodology. Skarbit et al. [30] summarized the LCZ air temperature measurements in four European cities. Until now, air temperature contrasts among different LCZs have not been studied at a continental scale.

In this study, we combine the LCZ map and ground-based air temperature measurements to conduct the first comparative analysis over China to address the following questions. Is there a consistent seasonal thermal contrast among different LCZs at the continental scale? How large is the air temperature variability within individual LCZs compared to the thermal contrast between different LCZs at the seasonal scale? Answers to these questions can advance our understanding of the relation between local landscape and air temperature and provide insights into the creation of cool neighborhoods and sustainable city development.

## 2. Materials and methods

### 2.1. Datasets

#### 2.1.1. Air temperature measurement

Hourly air temperature data measured at 1.5 m height above the ground level was collected from the national weather observation network by the National Meteorological Information Center of the China Meteorological Administration (<http://data.cma.cn/en>). Measurements at each site were made with platinum temperature sensors (QX/T-01 Chinese standard) housed in naturally ventilated Stevenson screens. The sensors have an uncertainty of  $\pm 0.2$  °C in the range of  $-50$  to  $+50$  °C. The data sets have been quality controlled and adopted to investigate the urbanization effect on air temperatures over China [39,40]. The spatial distribution of the weather stations is uneven across China (see Fig. 1), and less than 6% of the stations is truly rural stations away from urban areas [40]. Lin et al. [39] found that stations with a high urban surface fraction concentrated in coastal regions, while stations with a low urban surface fraction scattered throughout western China. In this study, for consistency with the LCZ map, we used the full year data of 2016 including 2131 stations. To look into thermal contrasts during the diurnal cycle, we defined daytime as 0900–1500 local time and nighttime as 2100–0300 local time. We defined seasons as follows, spring: March–May, summer: June–August, autumn: September–November, and winter: December–February.

#### 2.1.2. Local climate zone map

In this study, we utilized the 2016 LCZ map of China developed by Ren et al. [41] using an improved method of the World Urban Database and Portal Tool (WUDAPT) with Landsat satellite images. The overall accuracy of the LCZ map is 76% against ground truth samples [41]. This advanced method had also been applied for generating LCZ maps for Yangtze River Delta in China and its accuracy had been evaluated using mobile measurements [29,42]. The resultant LCZ map of China includes 10 built types (LCZ 1–10) and 7 land cover types (LCZ A–F) at a spatial resolution of 100 m  $\times$  100 m. It is noteworthy that built type LCZs are classified based on a set of landscape properties related to neighborhood planning and design. For example, the building surface fraction is used to separate 'compact' (40%–70%) and 'open' (20%–40%) neighborhoods, and the geometric average of building height is adopted to differentiate high-rise (>25 m), mid-rise (10 m–25 m), and low-rise (3 m–10 m) neighborhoods. Other classification parameters include sky view factor, aspect ratio, and impervious surface fraction. A detailed list of the surface parameters and their values for individual LCZ types can be found in Stewart and Oke [22].

### 2.2. Classification of meteorological stations

Locations of meteorological stations were overlaid with the LCZ map to classify the air temperature measurements into different LCZ types. Landscape homogeneity was checked to ensure measured data could represent characteristic air temperature regimes of different LCZ types. As the minimum radius to define LCZs is 200–500 m [22], we estimated the dominant LCZ types within  $3 \times 3$  grids and  $5 \times 5$  grids around each station. Only stations with two identical dominant LCZ types (i.e., within  $3 \times 3$  grids and  $5 \times 5$  grids) were considered in this study. By using both the  $3 \times 3$  and  $5 \times 5$  kernels, the station classification result will not be affected by 1 or 2 misclassified grid cells. However, there are inevitably potential errors due to the 76% overall accuracy of the adopted LCZ map, which may lead to errors in the subsequent comparisons. For comparing air temperature characteristics of LCZs at the continental scale, we excluded the LCZ types with insufficient number of stations (<40) or spatial span over China. To avoid bias introduced by a small number of stations with distinct geographical conditions, we focused on the area between 22° N and 40° N where the majority (95.9%) of built type LCZ stations fall (Fig. 1a). By controlling the landscape

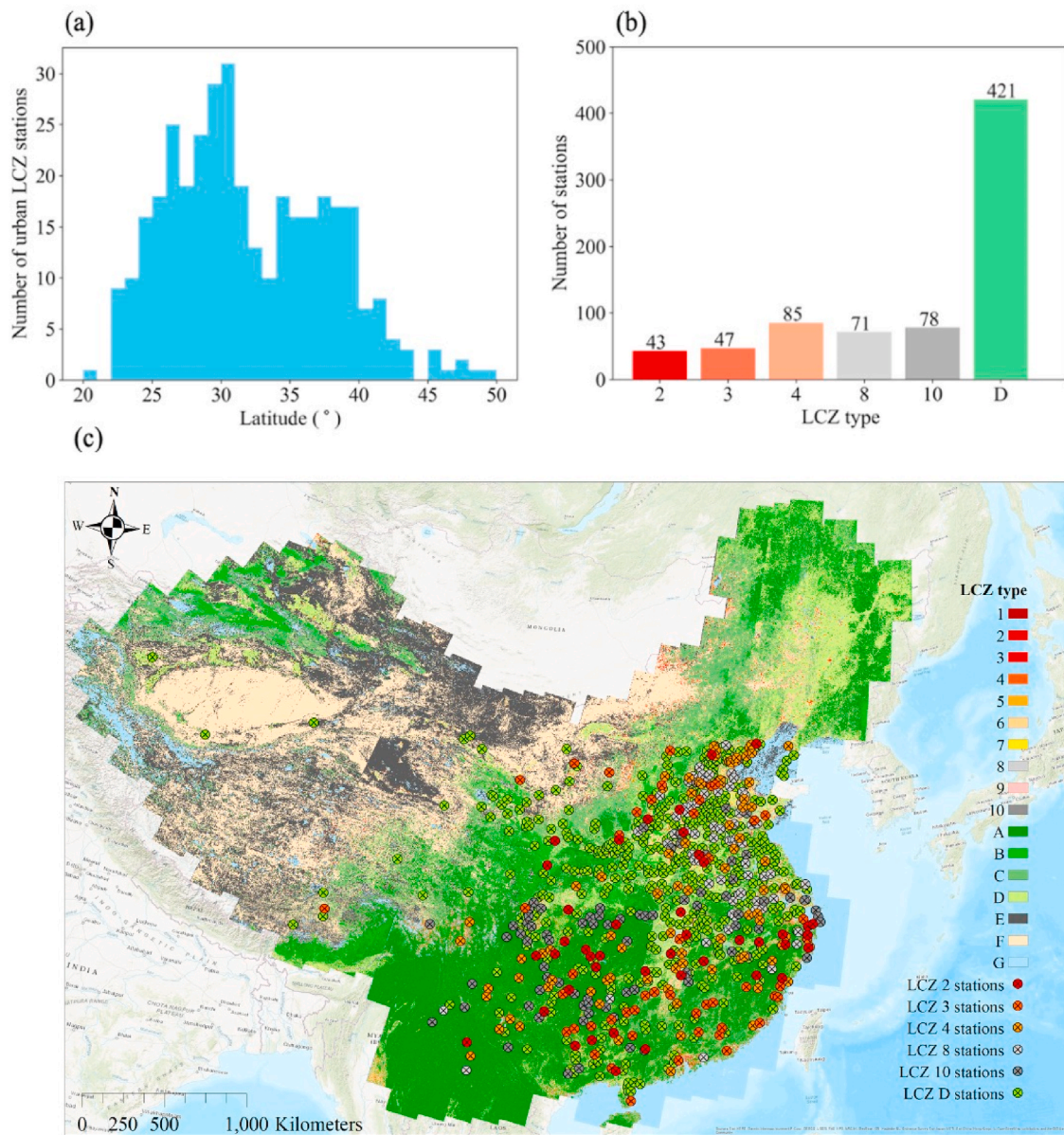


**Fig. 1.** Distribution of meteorological stations over China. (a) Latitude distribution of built type LCZ stations; (b) The number of stations in analyzed LCZ types in this study; (c) Spatial distribution of studied stations over the 2016 LCZ map of China. Land use types of LCZs: 2-Compact mid-rise, 3-Compact low-rise, 4-Open high-rise, 8-Large low-rise, 10-Heavy industry, D-Low plants.

homogeneity and station number, the impact of a few misclassified stations is minimized in our temperature analysis. In the end, a total of 745 stations from the 2131 stations collection were retained for analyses. Five urban LCZs (2: Compact mid-rise; 3: Compact low-rise; 4: Open high-rise; 8: Large low-rise; 10: Heavy industry) and one rural LCZ (D: Low plants) were selected. The number of stations for each LCZ type is shown in Fig. 1b. The spatial distribution of studied stations and the used LCZ map are shown in Fig. 1c. The elevation of the studied stations ranges from 1.3 m to over 3000 m.

### 2.3. Multiple linear regression for background air temperature

To estimate the thermal contrasts among different LCZs at the continental scale, the dependence of air temperature on geographical conditions must be removed. Daytime mean, nighttime mean, and daily mean temperatures for the 745 stations were calculated on a seasonal basis from the hourly data. Latitude (LAT), altitude (ALT) and the dis-

tance to coastline (DCL) are three critical parameters affecting the background mean air temperature [43]. A multiple regression model of the best fit was established using these three parameters as independent variables and air temperature as the dependent variable. The model was formulated as:

$$T_{pre} = \alpha_1LAT + \alpha_2ALT + \alpha_3DCL + \beta + \epsilon \tag{1}$$

where  $T_{pre}$  is the predicted background mean air temperature;  $\alpha_1$ ,  $\alpha_2$ , and  $\alpha_3$  are the coefficients for LAT, ALT, and DCL respectively;  $\beta$  is the intercept; and  $\epsilon$  is the residual. A regression model was built for each season separately using the data from all stations. Three different regression models for daytime mean, nighttime mean, and daily mean temperatures were built for each season. And each regression model was estimated based on 745 data points, corresponding to the number of meteorological stations.

2.4. Raw and standard thermal contrasts

To highlight the thermal contrast between various urban neighborhoods and the rural area, we set the low plants LCZ (type D) as the reference and computed the air temperature difference between built type LCZs ( $T_{ULCZ}$ ) and it:

$$\Delta T_r = \frac{\sum T_{ULCZ}}{n_{ULCZ}} - \frac{\sum T_D}{n_D} \quad (2)$$

where  $T_{ULCZ}$  and  $T_D$  are the measured seasonal mean air temperature at individual stations belong to built type LCZs and LCZ D;  $n_{ULCZ}$  and  $n_D$  denote the number of stations for each built type LCZ and LCZ D. We defined  $\Delta T_r$  as the raw thermal contrast, which had been employed in previous LCZ studies for city-scale analysis [29,44,45]. However,  $\Delta T_r$  can not reveal the ‘true’ thermal contrast among different LCZs at the continental scale, as observed air temperatures contain the signal of background mean temperature, which is determined by geographical conditions and is consequently biased by the spatial distribution of stations.

Using the regression model from Eq. (1), we removed the effect of geographical conditions to obtain the standard thermal contrast ( $\Delta T_s$ ). The usage of theoretical mean background temperature from the regression models bypass the selection of specific LCZ D stations, and allows the direct comparison of the standard seasonal thermal contrast at the continental scale. For each station, the impact of local landscapes was estimated as the deviation of measured air temperature from the predicted background mean air temperature. The deviation  $\Delta T_s$  for each station was given by:

$$\Delta T_s = T_{obs} - T_{pre} (LAT, ALT, DCL) \quad (3)$$

where  $T_{obs}$  is the observed seasonal mean air temperature, and  $T_{pre}$  is the predicted background seasonal mean air temperature from regression models that corresponds to the geographical condition of each station. Averaging  $\Delta T_s$  for all stations of one LCZ class would yield the characteristic air temperature regime of the LCZ with respect to the background air temperature. To be consistent with the raw thermal contrast ( $\Delta T_r$ ), we compared the mean values of standard thermal contrast between each built type LCZ and LCZ D ( $\Delta T_s^{ULCZ-D}$ ):

$$\Delta T_s^{ULCZ-D} = \frac{\sum \Delta T_s^{ULCZ}}{n_{ULCZ}} - \frac{\sum \Delta T_s^D}{n_D} \quad (4)$$

where  $\Delta T_s^{ULCZ}$  and  $\Delta T_s^D$  denote the standard seasonal thermal contrast for individual built type LCZ types and LCZ D (Eq. (3)), respectively. It is noteworthy that the impact of distance between built type LCZ stations and LCZ D stations is implicitly included in the multiple regression model. For example, latitude, altitude, and distance to coastline values will be very similar if the low plants area and built-up areas are close to each other. Thus, the method used in this study is not limited by the spatial distribution of the built type LCZ stations and LCZ D stations.

3. Results and discussion

3.1. Raw thermal contrast among LCZs

The monthly variation of daily mean air temperature for studied LCZ types is shown in Fig. 2a. Mean air temperature of all LCZs is about

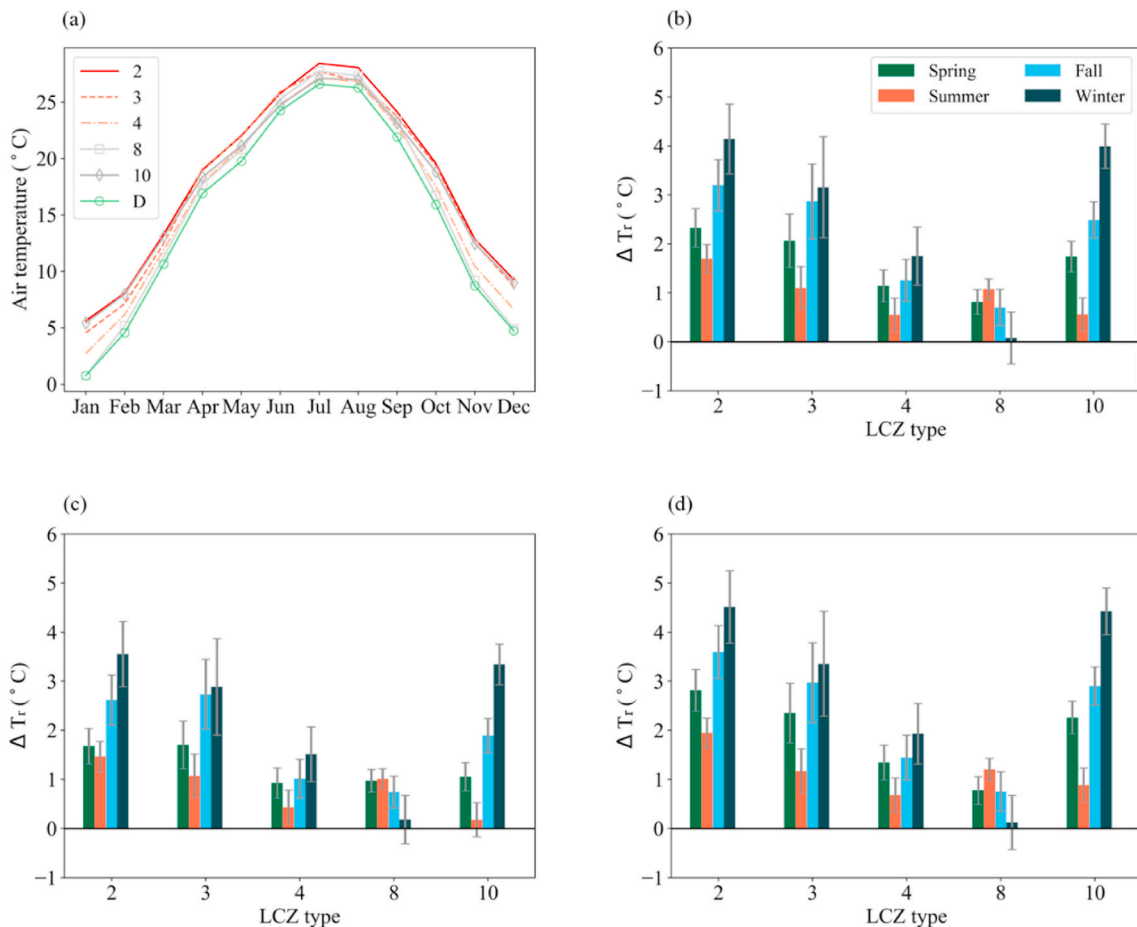


Fig. 2. (a) Monthly variation of daily mean air temperature over studied LCZ types; Raw (b) daily mean, (c) daytime mean, (d) nighttime mean thermal contrasts ( $\Delta T_r$ ) in four seasons over China. The error bar stands for one standard deviation from the mean.

26.6 °C in summer and 5.6 °C in winter. The air temperature variability among studied LCZs is the smallest in summer and the largest during winter. LCZ 2 has the highest air temperature throughout the year while LCZ D has the lowest air temperature. At the annual scale, the daily mean raw thermal contrast ( $\Delta T_r$ ) is  $1.8 \pm 0.5$  °C (mean  $\pm$  standard deviation among studied built type LCZs). Daily, daytime, and nighttime mean  $\Delta T_r$  in four seasons are shown in Fig. 2. Nighttime raw thermal contrasts (Fig. 2d) are found to be larger than daytime contrasts (Fig. 2c). Summertime daily mean  $\Delta T_r$  are lower than 2 °C over all LCZs, while wintertime daily mean  $\Delta T_r$  can reach up to 4 °C over LCZs 2 and 10 (Fig. 2b). Among the studied LCZs, compact mid-rise (LCZ 2) and heavy industry (LCZ 10) neighborhoods have the largest  $\Delta T_r$  and the large low-rise zone (LCZ 8) has the smallest  $\Delta T_r$ . The diurnal and seasonal variations of raw thermal contrasts here are consistent with previous studies, where urban-rural air temperature differences were found to be more evident in winter and during nighttime [30,46]. Nevertheless, results in Fig. 2 are biased by the unequal geographical conditions of stations in different LCZs. The raw thermal contrast thus cannot provide reliable estimations of the cooling potential if neighborhoods are to be redeveloped into other LCZ types.

### 3.2. Relation between air temperature and geographical conditions

For each season, one multiple linear regression model is built for daily mean, daytime mean and nighttime mean air temperatures, respectively. Fig. 3 shows the relations between geographical conditions and average daily mean air temperature in autumn over studied stations. Air temperatures are found to be negatively correlated with latitude, altitude, and the distance to coastline. Predicted daily mean air temperatures are compared against observations in Fig. 3d. It is clear that the linear regression model captures the observed air temperatures in autumn reasonably well with a  $R^2$  value of 0.95. Information of the regression models for all seasons is summarized in Table 1. In summer, autumn, and winter,  $R^2$  values are greater than 0.9 for all air temperatures with RMSEs less than 1.5 °C, indicating the capacity of built regression models in reproducing the relations between background mean air temperature and geographical conditions. Note that the regression coefficients for latitude, altitude and the distance to coastline have considerable seasonal variations. Daily mean air temperature reduces about 1 °C per degree latitude in winter but reduces only about 0.2 °C per degree latitude in summer. Daytime mean air temperature tends to decrease with the distance to coastline in autumn but would

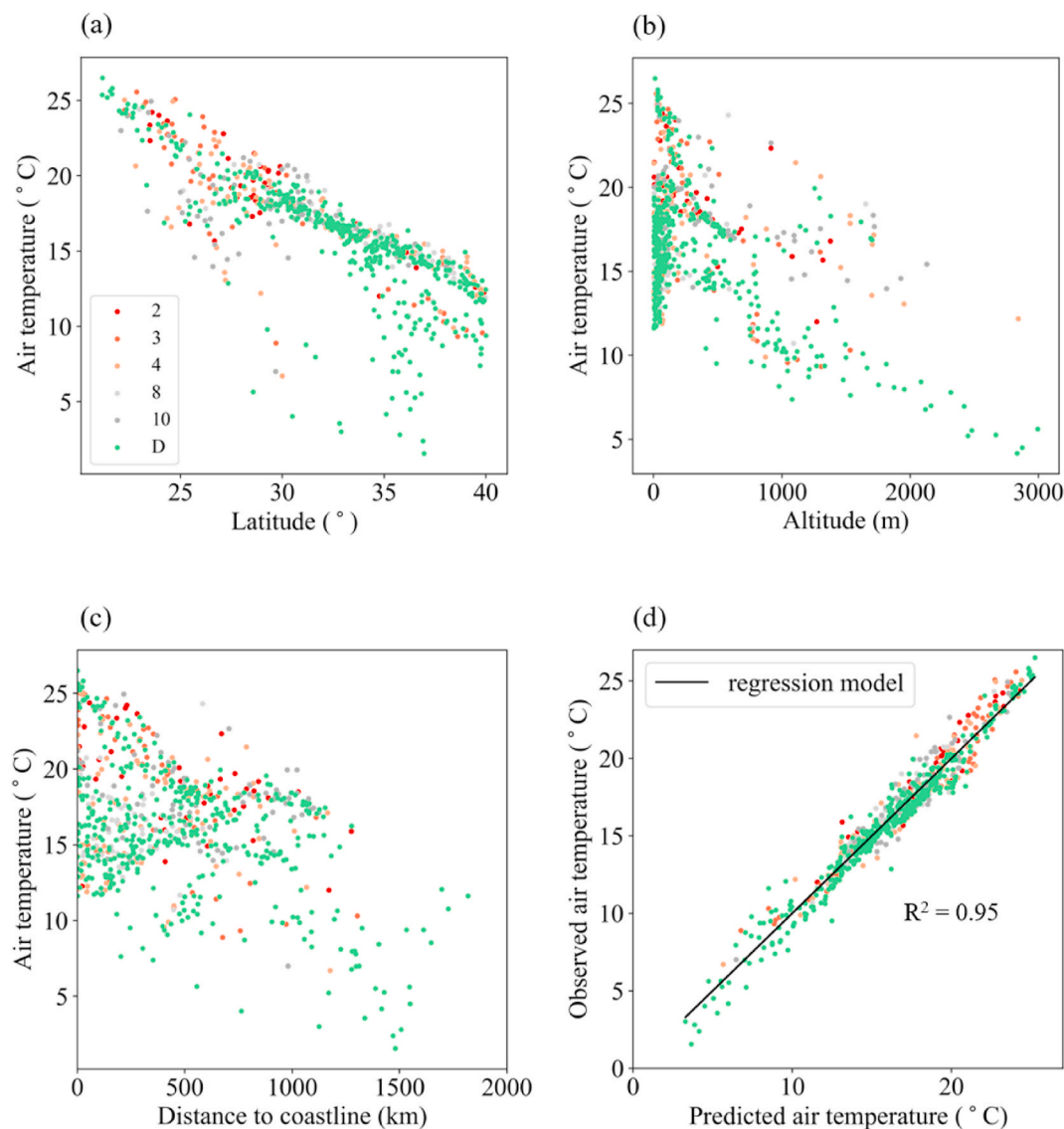


Fig. 3. Relationship between (a) latitude, (b) altitude, (c) distance to the coastline and daily mean air temperature in autumn; (d) comparison of predicted daily mean air temperature against observations in autumn.

**Table 1**

Summary of regression models for daily mean, daytime (0900–1500 local time) mean, and nighttime (2100–0300 local time) mean air temperatures in four seasons.

Daily mean air temperature					
	LAT coefficient (°C/degree)	ALT coefficient (°C/km)	DCL coefficient (°C/km)	R <sup>2</sup>	Root mean square error (°C)
Spring	-0.45	-3.30	$1.27 \times 10^{-3}$	0.81	1.35
Summer	-0.19	-4.44	$1.59 \times 10^{-3}$	0.93	0.73
Autumn	-0.68	-3.42	$-0.07 \times 10^{-3}$	0.95	0.89
Winter	-1.02	-3.05	$1.26 \times 10^{-3}$	0.95	1.20
Daytime mean air temperature					
Spring	-0.32	-3.08	$0.37 \times 10^{-3}$	0.73	1.47
Summer	-0.15	-4.39	$1.24 \times 10^{-3}$	0.92	0.78
Autumn	-0.59	-3.13	$-0.90 \times 10^{-3}$	0.94	0.92
Winter	-0.92	-2.94	$0.39 \times 10^{-3}$	0.94	1.18
Nighttime mean air temperature					
Spring	-0.54	-3.46	$1.73 \times 10^{-3}$	0.84	1.36
Summer	-0.23	-4.49	$1.67 \times 10^{-3}$	0.93	0.84
Autumn	-0.74	-3.70	$0.28 \times 10^{-3}$	0.95	0.99
Winter	-1.08	-3.24	$1.58 \times 10^{-3}$	0.94	1.31

increase with the distance in other seasons. Though we have not explicitly included meteorological variables in the regression analysis, the seasonal variation of regression models implicitly contains the impact of inter-season change in meteorological conditions on background mean air temperature.

### 3.3. Standard thermal contrast among LCZs

As  $\Delta T_s$  denotes the deviation from background mean air temperature, it is a good indicator for examining whether the impact of local urban landscape varies with geographical conditions. Results for nighttime air temperature over LCZ 2 (compact mid-rise) in four seasons are shown in Fig. 4. Stations in the compact mid-rise LCZ have air temperature differences mainly in the range of  $-1$  to  $3$  °C relative to the background mean air temperature. Fig. 5 shows that daytime  $\Delta T_s$  over LCZ 10 (heavy industry) falls within the range of  $-2$  to  $3$  °C throughout the year. Comparing Figs. 4 and 5, the largest difference is found in summertime, where nighttime  $\Delta T_s$  in LCZ 2 has more positive values than daytime  $\Delta T_s$  in LCZ 10. The variation in  $\Delta T_s$  over each LCZ is partially caused by the LCZ scheme that landscape properties fall within a wide range when classifying LCZ types. Despite the large variation,  $\Delta T_s$  does not have a statistically significant correlation with changes in latitude, altitude, and the distance to coastline. Same conclusion can be made for daytime, nighttime, and daily mean  $\Delta T_s$  values over other studied LCZs (results not shown here). Note that the large variation here is not much larger than values reported in previous studies at the city scale [30,31,47]. Take the study in Nanjing, China as an example [31], nighttime  $\Delta T_s$  were found to vary between 1 and 5 °C for LCZ 2 and between  $-1$ – $3$  °C for LCZ 8.

Besides the local urban effect, the  $\Delta T_s$  here unavoidably contains information of small-scale topographic variations, such as valleys and ridges. These topographic variations have notable impacts on air temperature, e.g., cold air drainage in valleys [48], but cannot be detected in the regression models built on latitude, altitude, and the distance to coastline. Upwind and downwind areas also play a role in affecting the  $\Delta T_s$  [35]. These could be some of the reasons that  $\Delta T_s$  has a large variation in each season (see Figs. 4 and 5). Other climatic influences that do not correlate with latitude, altitude, or the distance to coastline may also shift the distribution patterns of the  $\Delta T_s$  spatially and temporally. For example, the Yangtze river delta region in China experiences a long period of steady rainfall during the monsoon season [49]. The rainfall period can affect the soil moisture and subsequently the air temperature. Such time- and site-specific events will modify the  $\Delta T_s$  of

some stations in one LCZ type but not the others. The multiple linear regression models in this study are not able to capture these climatic influences.

Fig. 6 shows the average daily, daytime and nighttime  $\Delta T_s^{\text{ULCZ-D}}$  in four seasons over China. Compared to Fig. 2, it is clear that  $\Delta T_s^{\text{ULCZ-D}}$  are smaller than raw thermal contrasts, with all values below 1 °C. The  $\Delta T_s^{\text{ULCZ-D}}$  values represent the differences of local urban effect on the air temperature between built type LCZs and LCZ D. Annual mean  $\Delta T_s^{\text{ULCZ-D}}$  is found to be larger at night ( $0.5 \pm 0.2$  °C, mean  $\pm$  standard deviation among studied built type LCZs, Fig. 6c) than during daytime ( $0.2 \pm 0.2$  °C, Fig. 6b). For nighttime air temperature in winter, the maximum  $\Delta T_s^{\text{ULCZ-D}}$  of about 0.8 °C is found over LCZ 10 (heavy industry) and the minimum  $\Delta T_s^{\text{ULCZ-D}}$  is found over LCZ 3 (compact low-rise). Contrarily, large daytime thermal contrasts are observed over LCZ 3 in summer, while a small negative value occurs over LCZ 10. Daily mean  $\Delta T_s^{\text{ULCZ-D}}$  remain relatively constant across four seasons over LCZ 2 (compact mid-rise) with values around 0.5 °C. Results here clearly demonstrate the different behaviors of characteristic air temperature regimes over studied LCZ types in response to seasonal and diurnal variations of meteorological conditions.

We would like to point out that mean variation of  $\Delta T_s^{\text{ULCZ-D}}$  within individual LCZs is 0.2 °C (error bars in Fig. 6), which is as large as the standard deviation of  $\Delta T_s^{\text{ULCZ-D}}$  among studied 5 built LCZ types. This indicates that when one LCZ has higher mean air temperatures than others, some stations belong to that LCZ could have lower air temperatures. Such variation was partly due to the structure of the LCZ system, where the ranges of landscape properties used for classifying different LCZs overlap. For example, LCZ 2 and LCZ 3 have the same building surface fraction range (40%–70%) and a similar aspect ratio range (0.75–2 for LCZ 2 and 0.75–1.5 for LCZ 3). Though many other parameters are involved in the LCZ classification scheme, overlapped ranges inevitably result in the large variability in the characteristic air temperature regime of LCZs and consequently their thermal contrast.

In spite of the considerable variation, standard thermal contrasts among different LCZs estimated in this study support the validity of the LCZ scheme at the continental scale. Though the magnitudes of standard seasonal thermal contrasts are not large, we would like to emphasize that estimated  $\Delta T_s$  represent the influence on air temperature solely by local urban landscape and do not vary with geographical conditions. Using observed air temperature data in 2016, we find the annual mean air temperature over studied built type LCZs is 0.4 °C higher than that over the areas with low plants.

### 3.4. Implications for cool neighborhoods

Estimated standard thermal contrasts ( $\Delta T_s^{\text{ULCZ-D}}$ ) in Fig. 6 have important implications for design and planning of cool neighborhoods. The LCZs 8 (large low-rise) and 10 (heavy industry) are mainly industrial areas within cities and thus they are not key elements in cool cities. In compact built environment, Fig. 6 shows that mid-rise neighborhoods (LCZ 2) have higher nighttime air temperatures and lower daytime air temperatures than low-rise neighborhoods (LCZ 3) over China. The reason is that low building heights lead to small shading effects during daytime and have limited heat trapping effects at night. Nevertheless, summer  $\Delta T_s^{\text{ULCZ-D}}$  is considerably higher in LCZs 2 and 3 than in other built type LCZs, which demonstrates the need for heat mitigation in compact neighborhoods. As buildings occupy 40–70% of the land surface in compact neighborhoods, surface retrofitting with novel engineering materials is a potential heat mitigation strategy that does not require reforming building morphology. In terms of creating sustainable neighborhoods, the open high-rise neighborhood (LCZ 4) will be recommended: it has relatively low  $\Delta T_s^{\text{ULCZ-D}}$  in both daytime and nighttime, and its higher thermal contrast during winter than in summer is desirable [50,51]. On top of this, open high-rise neighborhoods could have similar population density with compact mid-rise or low-rise neighborhoods, which makes them preferable for both efficient space

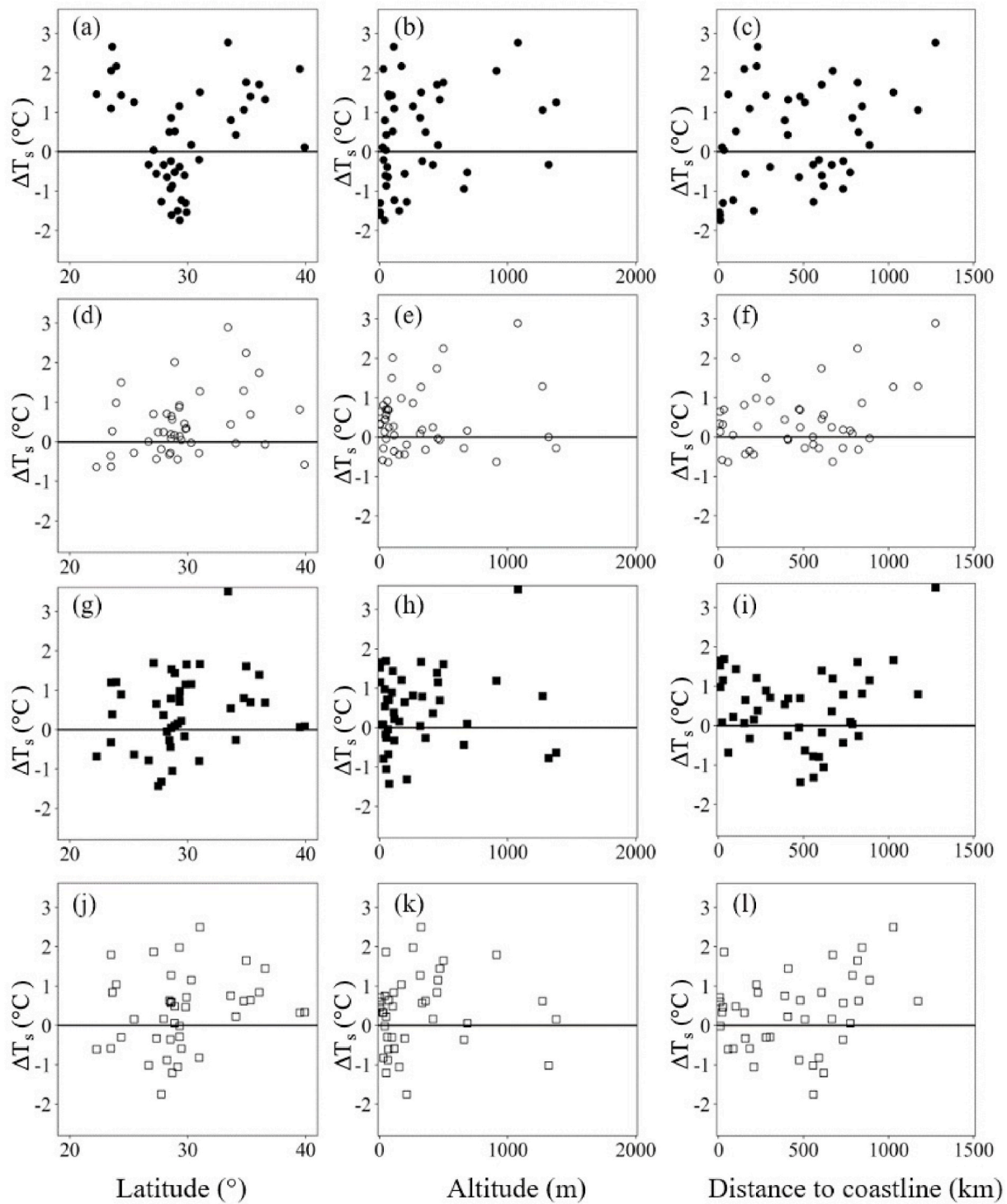


Fig. 4. Distribution of the nighttime thermal contrast ( $\Delta T_s$ ) over latitude, altitude and distance to coastline over LCZ 2 in (a)–(c) spring, (d)–(f) summer, (g)–(i) autumn, and (j)–(l) winter.

utilization and comfort thermal environment.

#### 4. Conclusion

In this study, we make the first attempt to examine the characteristic seasonal air temperature regimes of different LCZs across China. Using the areas with low plants as the reference LCZ type, estimated raw thermal contrasts directly from station measurements are found to be up to 4 °C in winter. After removing the signal of background mean air

temperature, the standard thermal contrasts become less than 1 °C for all seasons. Results show that the warmth of built type LCZs is more evident during nighttime, with the maximum effect observed in compact mid-rise zones. The impact of local urban landscape on air temperature over studied LCZ types are consistent at the continental scale and do not change with geographical conditions. Large standard thermal contrast with low variations suggests consistently high air temperatures in compact mid-rise neighborhoods (LCZ 2) throughout the year. On the other hand, open high-rise neighborhoods (LCZ 4) have relatively large

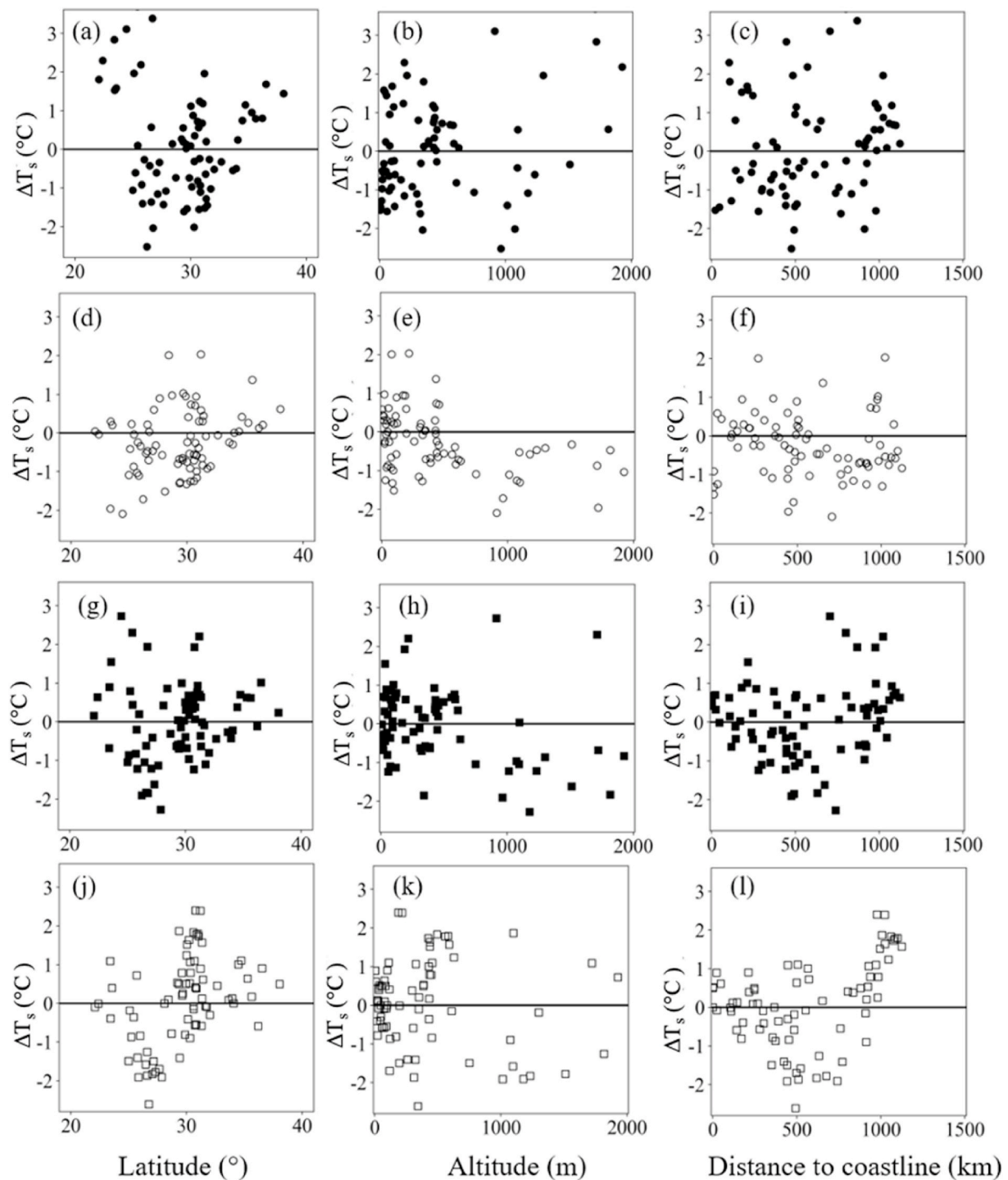


**Fig. 5.** Distribution of the daytime thermal contrast ( $\Delta T_s$ ) over latitude, altitude and distance to coastline over LCZ 10 in (a)–(c) spring, (d)–(f) summer, (g)–(i) autumn, and (j)–(l) winter.

$\Delta T_s$  in winter and overall low  $\Delta T_s$  in summer, which is desirable in terms of building energy consumption and outdoor thermal comfort. Estimated standard thermal contrasts in this study are generalizable for neighborhoods in a variety of Chinese cities without in-situ observations. Our study investigates the thermal contrast at sub-kilometer scales, and thus findings could provide guidance for neighborhood design and planning to create cool cities and communities.

The reduction in sensor cost and the ease of data communication have allowed us to monitor the urban thermal environment at a much finer resolution [52]. A recent study showed the critical role of

intra-urban climate variability on modifying residents' health risk under extreme events [53]. The LCZ system provides a good standard for classifying urban neighborhoods with heterogeneous landscape and facilitates the design and development of urban monitoring networks. The methodology used to derive the standard seasonal thermal contrast in this study can also be extended to the global scale in future studies, subject to the availability of LCZ map and surface meteorological dataset. Due to data availability, our analysis only focuses on air temperature. Future studies shall investigate the characteristic regime of other meteorological variables over different LCZs, such as air humidity

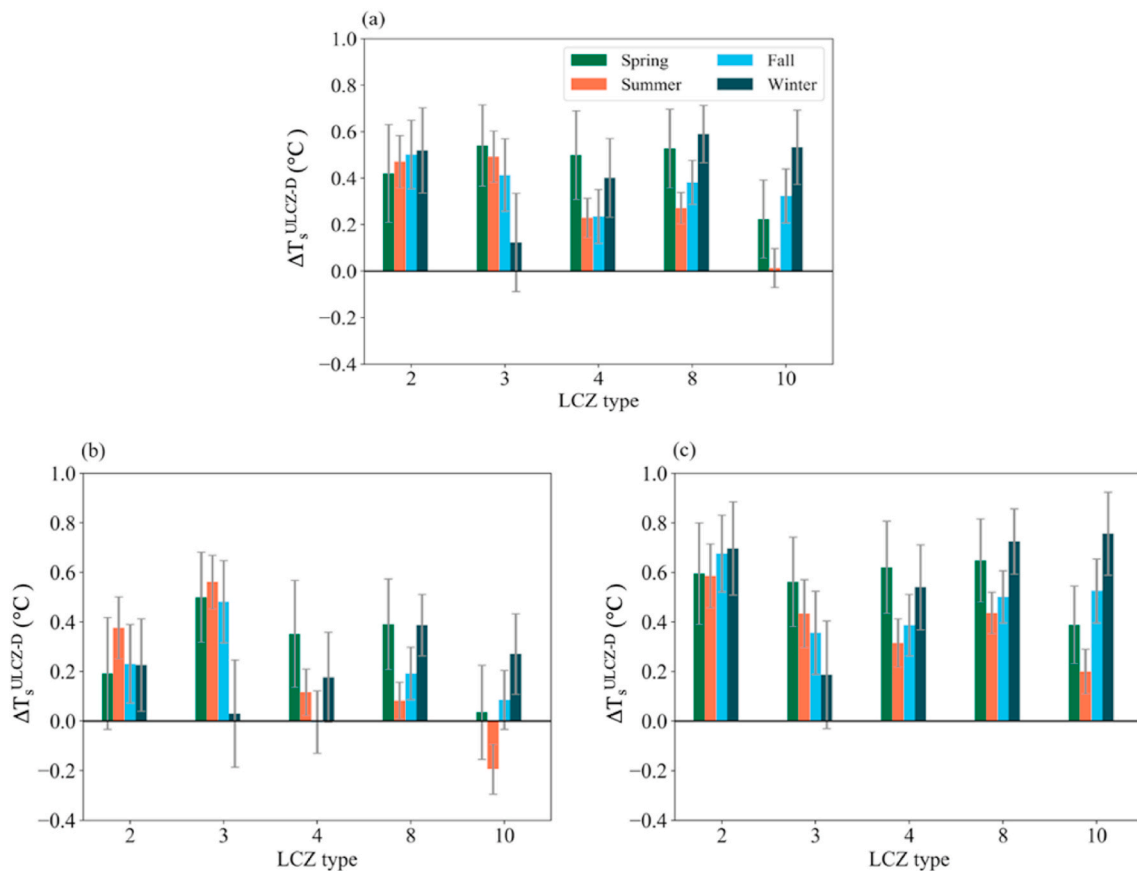


**Fig. 6.** Standard (a) daily mean, (b) daytime mean, (c) nighttime mean thermal contrast ( $\Delta T_s^{ULCZ-D}$ ) in four seasons over China. The error bar stands for one standard deviation from the mean.

and wind speed. Due to the limitation of the built regression models, estimated standard thermal contrast inevitably contains information of small-scale topographic variation and climatic influence, whose effects are not captured by the latitude, altitude and the distance to coastline. As a result, the standard seasonal thermal contrasts for studied LCZ types have a large variation. The relation between air temperature variability and small-scale topography as well as meteorological conditions in different LCZs is worth further investigation.

#### Declaration of competing interest

The authors declare that they have no known competing financial interests or personal relationships that could have appeared to influence the work reported in this paper.

#### Acknowledgement

This work was supported by the Hong Kong Research Grants Council funded project 16204220. Due to data policy in China, original hourly air temperature data at 2131 stations are not available via a public repository. Anyone of interest could contact China Meteorological Administration (<http://data.cma.cn/en>) for detailed information of data acquisition. Seasonal daily, daytime and nighttime mean air temperature data in this study is available at: <https://doi.org/10.5281/zenodo.3940212>. The study of LCZ data development was partially supported by the Vice-Chancellor's One-off Discretionary Fund of The Chinese University of Hong Kong.

#### References

- [1] T.R. Oke, The energetic basis of the urban heat island, *Q. J. R. Meteorol. Soc.* 108 (455) (1982) 1–24, <https://doi.org/10.1002/qj.49710845502>.
- [2] L. Howard, *The Climate of London: Deduced from Meteorological Observations Made in the Metropolis and at Various Places Around it*, vol. 3, Harvey and Darton, London, 1833.
- [3] M. Santamouris, C. Cartalis, A. Synnefa, D. Kolokotsa, On the impact of urban heat island and global warming on the power demand and electricity consumption of buildings—a review, *Energy Build.* 98 (2015) 119–124, <https://doi.org/10.1016/j.enbuild.2014.09.052>.
- [4] C.J. Tomlinson, L. Chapman, J.E. Thornes, C.J. Baker, Including the urban heat island in spatial heat health risk assessment strategies: a case study for Birmingham, UK, *Int. J. Health Geogr.* 10 (1) (2011) 42, <https://doi.org/10.1186/1476-072X-10-42>.
- [5] A. Barreca, K. Clay, O. Deschenes, M. Greenstone, J.S. Shapiro, Adapting to climate change: the remarkable decline in the US temperature-mortality relationship over the twentieth century, *J. Polit. Econ.* 124 (1) (2016) 105–159, <https://doi.org/10.1086/684582>.
- [6] X. Chen, S.J. Jeong, Shifting the urban heat island clock in a megacity: a case study of Hong Kong, *Environ. Res. Lett.* 13 (1) (2018), 014014, <https://doi.org/10.1088/1748-9326/aa95fb>.
- [7] G. Levermore, J. Parkinson, K. Lee, P. Laycock, S. Lindley, The increasing trend of the urban heat island intensity, *Urban Climate* 24 (2018) 360–368, <https://doi.org/10.1016/j.uclim.2017.02.004>.
- [8] F.S. Palou, A. Mahalov, Summer-and wintertime variations of the surface and near-surface urban heat island in a semiarid environment, *Weather Forecast.* 34 (6) (2019) 1849–1865, <https://doi.org/10.1175/WAF-D-19-0054.1>.
- [9] P.K. Cheung, C.Y. Jim, Effects of urban and landscape elements on air temperature in a high-density subtropical city, *Build. Environ.* 164 (2019) 106362, <https://doi.org/10.1016/j.buildenv.2019.106362>.
- [10] M. Santamouris, Cooling the cities—a review of reflective and green roof mitigation technologies to fight heat island and improve comfort in urban environments, *Sol. Energy* 103 (2014) 682–703, <https://doi.org/10.1016/j.solener.2012.07.003>.
- [11] M.S. Wong, J.E. Nichol, P.H. To, J. Wang, A simple method for designation of urban ventilation corridors and its application to urban heat island analysis, *Build. Environ.* 45 (8) (2010) 1880–1889, <https://doi.org/10.1016/j.buildenv.2010.02.019>.
- [12] J. Yang, Z.H. Wang, K.E. Kaloush, H. Dylla, Effect of pavement thermal properties on mitigating urban heat islands: a multi-scale modeling case study in Phoenix,

- Build. Environ. 108 (2016) 110–121, <https://doi.org/10.1016/j.buildenv.2016.08.021>.
- [13] X. Yang, L.L. Peng, Z. Jiang, Y. Chen, L. Yao, Y. He, T. Xu, Impact of urban heat island on energy demand in buildings: local climate zones in Nanjing, Appl. Energy 260 (2020) 114279, <https://doi.org/10.1016/j.apenergy.2019.114279>.
- [14] A. Martilli, E.S. Krayenhoff, N. Nazarian, Is the urban heat island intensity relevant for heat mitigation studies? Urban Climate 31 (2020) 100541, <https://doi.org/10.1016/j.uclim.2019.100541>.
- [15] T.R. Oke, Initial Guidance to Obtain Representative Meteorological Observations at Urban Sites. IOM Report, vol. 81, World Meteorological Organization, Geneva, 2006.
- [16] E. Fukui, T. Wada, Horizontal distribution of the air temperature in greater cities of Japan, In Japanese, Geogr. Rev. Jpn. 17 (5) (1941) 354–372, <https://doi.org/10.4157/grj.17.354>.
- [17] W. Schmidt, Die verteilung der minimumtemperaturen in der frostnacht des 12 Mai 1927 im gemeindegebiet von Wien. [Distribution of minimum temperatures during the frost night of May 12, 1927, within the communal limits of Vienna], Fortschritte der Landwirtschaft 2 (21) (1927) 681–686.
- [18] Å. Sundborg, Climatological studies in Uppsala: with special regard to the temperature conditions in the urban area, in: Geographica vol. 22, Geographical Institute of Uppsala, Sweden, 1951.
- [19] Iain D. Stewart, Why should urban heat island researchers study history? Urban Climate 30 (2019) 100484, <https://doi.org/10.1016/j.uclim.2019.100484>.
- [20] C.L. Muller, L. Chapman, C.S.B. Grimmond, D.T. Young, X. Cai, Sensors and the city: a review of urban meteorological networks, Int. J. Climatol. 33 (7) (2013) 1585–1600, <https://doi.org/10.1002/joc.3678>.
- [21] P. Ramamurthy, J. González, L. Ortiz, M. Arend, F. Moshary, Impact of heatwave on a megacity: an observational analysis of New York City during July 2016, Environ. Res. Lett. 12 (5) (2017), 054011, <https://doi.org/10.1088/1748-9326/aa6e59>.
- [22] I.D. Stewart, T.R. Oke, Local climate zones for urban temperature studies, Bull. Am. Meteorol. Soc. 93 (12) (2012) 1879–1900, <https://doi.org/10.1175/BAMS-D-11-00019.1>.
- [23] M. Anjos, A.C. Targino, P. Krecel, G.Y. Oukawa, R.F. Braga, Analysis of the urban heat island under different synoptic patterns using local climate zones, Build. Environ. 185 (2020) 107268, <https://doi.org/10.1016/j.buildenv.2020.107268>.
- [24] D. Fenner, F. Meier, B. Bechtel, M. Otto, D. Scherer, Intra and inter local climate zone variability of air temperature as observed by crowdsourced citizen weather stations in Berlin, Germany, Meteorol. Z. 26 (2017) 525–547, <https://doi.org/10.1127/metz/2017/0861>.
- [25] K.K.-L. Lau, S.C. Chung, C. Ren, Outdoor thermal comfort in different urban settings of sub-tropical high-density cities: an approach of adopting local climate zone (LCZ) classification, Build. Environ. 154 (2019) 227–238, <https://doi.org/10.1016/j.buildenv.2019.03.005>.
- [26] I.D. Stewart, T.R. Oke, E.S. Krayenhoff, Evaluation of the 'local climate zone' scheme using temperature observations and model simulations, Int. J. Climatol. 34 (4) (2014) 1062–1080, <https://doi.org/10.1002/joc.3746>.
- [27] C. Wang, A. Middel, S.W. Myint, S. Kaplan, A.J. Brazel, J. Lukasczyk, Assessing local climate zones in arid cities: the case of Phoenix, Arizona and Las Vegas, Nevada, ISPRS J. Photogrammetry Remote Sens. 141 (2018) 59–71, <https://doi.org/10.1016/j.isprsjprs.2018.04.009>.
- [28] P.J. Alexander, G. Mills, Local climate classification and Dublin's urban heat island, Atmosphere 5 (4) (2014) 755–774, <https://doi.org/10.3390/atmos5040755>.
- [29] Y. Shi, K.K. Lau, C. Ren, E. Ng, Evaluating the local climate zone classification in high-density heterogeneous urban environment using mobile measurement, Urban Climate 25 (2018) 167–186, <https://doi.org/10.1016/j.uclim.2018.07.001>.
- [30] N. Skarbit, I.D. Stewart, J. Unger, T. Gál, Employing an urban meteorological network to monitor air temperature conditions in the 'local climate zones' of Szeged, Hungary, Int. J. Climatol. 37 (2017) 582–596, <https://doi.org/10.1002/joc.5023>.
- [31] X. Yang, L. Yao, T. Jin, L.L. Peng, Z. Jiang, Z. Hu, Y. Ye, Assessing the thermal behavior of different local climate zones in the Nanjing metropolis, China, Build. Environ. 137 (2018) 171–184, <https://doi.org/10.1016/j.buildenv.2018.04.009>.
- [32] I.D. Stewart, A systematic review and scientific critique of methodology in modern urban heat island literature, Int. J. Climatol. 31 (2) (2011) 200–217, <https://doi.org/10.1002/joc.2141>.
- [33] T.R. Oke, Towards better scientific communication in urban climate, Theor. Appl. Climatol. 84 (1–3) (2006) 179–190, <https://doi.org/10.1007/s00704-005-0153-0>.
- [34] U. Wienert, W. Kuttler, The dependence of the urban heat island intensity on latitude—a statistical approach, Meteorol. Z. 14 (5) (2005) 677–686, <https://doi.org/10.1127/0941-2948/2005/0069>.
- [35] W.P. Lowry, Empirical estimation of urban effects on climate: a problem analysis, J. Appl. Meteorol. Climatol. 16 (2) (1977) 129–135, [https://doi.org/10.1175/1520-0450\(1977\)016<0129:EEOUEO>2.0.CO;2](https://doi.org/10.1175/1520-0450(1977)016<0129:EEOUEO>2.0.CO;2).
- [36] J. Unger, N. Skarbit, T. Gál, Evaluation of outdoor human thermal sensation of local climate zones based on long-term database, Int. J. Biometeorol. 62 (2) (2018) 183–193, <https://doi.org/10.1007/s00484-017-1440-z>.
- [37] R. Wang, W. Gao, N. Zhou, D.M. Kammen, W. Peng, Urban structure and its implication of heat stress by using remote sensing and simulation tool, Sustain. Cities Soc. (2020) 102632, <https://doi.org/10.1016/j.scs.2020.102632>.
- [38] X. Zhou, T. Okaze, C. Ren, M. Cai, Y. Ishida, H. Watanabe, A. Mochida, Evaluation of urban heat islands using local climate zones and the influence of sea-land breeze, Sustain. Cities Soc. 55 (2020) 102060, <https://doi.org/10.1016/j.scs.2020.102060>.
- [39] L. Lin, M. Luo, T.O. Chan, E. Ge, X. Liu, Y. Zhao, W. Liao, Effects of urbanization on winter wind chill conditions over China, Sci. Total Environ. 688 (2019) 389–397, <https://doi.org/10.1016/j.scitotenv.2019.06.145>.
- [40] Y. Sun, X. Zhang, G. Ren, F.W. Zwiers, T. Hu, Contribution of urbanization to warming in China, Nat. Clim. Change 6 (7) (2016) 706–709, <https://doi.org/10.1038/nclimate2956>.
- [41] C. Ren, M. Cai, X. Li, L. Zhang, R. Wang, Y. Xu, E. Ng, Assessment of local climate zone classification maps of cities in China and feasible refinements, Sci. Rep. 9 (1) (2019) 18848, <https://doi.org/10.1038/s41598-019-55444-9>.
- [42] M. Cai, C. Ren, Y. Xu, K.K. Lau, R. Wang, Investigating the relationship between local climate zone and land surface temperature using an improved WUDAPT methodology—A case study of Yangtze river delta, China, Urban Climate 24 (2018) 485–502, <https://doi.org/10.1016/j.uclim.2017.05.010>.
- [43] E. Linacre, B. Geerts, Climates and Weather Explained, Routledge, Abingdon, 1997.
- [44] R. Kotharkar, A. Bagade, Evaluating urban heat island in the critical local climate zones of an Indian city, Landsc. Urban Plann. 169 (2018) 92–104, <https://doi.org/10.1016/j.landurbplan.2017.08.009>.
- [45] M. Verdonck, M. Demuzere, H. Hooyberghs, C. Beck, J. Cyrys, A. Schneider, F. Van Coillie, The potential of local climate zones maps as a heat stress assessment tool, supported by simulated air temperature data, Landsc. Urban Plann. 178 (2018) 183–197, <https://doi.org/10.1016/j.landurbplan.2018.06.004>.
- [46] D. Zhou, S. Zhao, S. Liu, L. Zhang, C. Zhu, Surface urban heat island in China's 32 major cities: spatial patterns and drivers, Rem. Sens. Environ. 152 (2014) 51–61, <https://doi.org/10.1016/j.rse.2014.05.017>.
- [47] J. Geletić, M. Lehnert, P. Dobrovolný, Land surface temperature differences within local climate zones, based on two central European cities, Rem. Sens. 8 (10) (2016) 788, <https://doi.org/10.3390/rs8100788>.
- [48] C. Daly, D.R. Conklin, M.H. Unsworth, Local atmospheric decoupling in complex topography alters climate change impacts, Int. J. Climatol. 30 (12) (2010) 1857–1864, <https://doi.org/10.1002/joc.2007>.
- [49] Y. Ding, P. Liang, Y. Liu, Y. Zhang, Multiscale variability of meiyu and its prediction: a new review, J. Geophys. Res.: Atmosphere 125 (7) (2020), <https://doi.org/10.1029/2019JD031496>.
- [50] J. Yang, E. Bou-Zeid, Should cities embrace their heat islands as shields from extreme cold? J. Appl. Meteorol. Climatol. 57 (6) (2018) 1309–1320, <https://doi.org/10.1175/JAMC-D-17-0265.1>.
- [51] Z. Yang, Y. Chen, Z. Zheng, Q. Huang, Z. Wu, Application of building geometry indexes to assess the correlation between buildings and air temperature, Build. Environ. 167 (2020) 106477, <https://doi.org/10.1016/j.buildenv.2019.106477>.
- [52] J. Yang, E. Bou-Zeid, Designing sensor networks to resolve spatio-temporal urban temperature variations: fixed, mobile or hybrid? Environ. Res. Lett. 14 (7) (2019) <https://doi.org/10.1088/1748-9326/ab25f8>, 074022.
- [53] J. Yang, L. Hu, C. Wang, Population dynamics modify urban residents' exposure to extreme temperatures across the United States, Sci. Adv. 5 (12) (2019), <https://doi.org/10.1126/sciadv.aay3452> eaay3452.